SCIENCE CHINA
Earth Sciences

•ARTICLE•

September 2024 Vol.67 No.9: 2937–2952
https://doi.org/10.1007/s11430-023-1335-8

Vegetation changes across the Eocene-Oligocene transition: Global signals vs. regional development

Mengxiao WU[1,2], Lutz KUNZMANN[2*], Shufeng LI[1], Vasilis TEODORIDIS[3], Zhekun ZHOU[1] & Tao SU[1,4,5*]

[1] *CAS Key Laboratory of Tropical Forest Ecology, Xishuangbanna Tropical Botanical Garden, Chinese Academy of Sciences, Mengla 666303, China;*
[2] *Senckenberg Natural History Collections Dresden, Königsbrücker Landstraße 159, Dresden 01109, Germany;*
[3] *Department of Biology and Environmental Studies, Faculty of Education, Charles University, Magdalény Rettigové 4, 116 39 Prague 1, Czech Republic;*
[4] *State Key Laboratory of Oil and Gas Reservoir Geology and Exploitation, Chengdu University of Technology, Chengdu 610059, China;*
[5] *Institute of Sedimentary Geology, Chengdu University of Technology, Chengdu 610059, China*

Received September 26, 2023; revised April 1, 2024; accepted May 10, 2024; published online August 7, 2024

Abstract The Eocene-Oligocene transition (EOT) marked a rapid global cooling event, often considered as the beginning of the modern icehouse world. Influenced by various factors, including tectonic activity and paleogeographic settings, the terrestrial records indicate a diverse response of fauna and vegetation to this global event. We examined nine macrofossil assemblages from seven fossil localities on the southeastern margin of the Tibetan Plateau and from the mid-latitudinal Europe ranging from the latest Bartonian and Priabonian (37.71–33.9 Ma) to the Rupelian (33.9–27.82 Ma). Our aims were to trace and compare the vegetation history of both regions in the late Eocene and early Oligocene. The results show that both regions experienced changes in vegetation composition in response to climate change, characterized by a decrease in the percentages of broad-leaved evergreen elements and distinctive changes in general vegetation types. A general change in the overall vegetation type from subtropical broad-leaved evergreen forests in the late Eocene to temperate broad-leaved mixed deciduous evergreen forests, or mixed mesophytic forests, in the early Oligocene is recognized in both regions. The results indicate a clear change in leaf architecture, leaf margin states, and secondary venation types in the mid-latitudinal Europe, while the results from the southeastern margin of the Tibetan Plateau show a distinct reduction in leaf size. Our data suggest that both global and regional factors played key roles in shaping the vegetation in the two regions.

Keywords Eocene-Oligocene transition, Plant fossil, Paleoclimate, Leaf architecture, Biodiversity

Citation: Wu M, Kunzmann L, Li S, Teodoridis V, Zhou Z, Su T. 2024. Vegetation changes across the Eocene-Oligocene transition: Global signals vs. regional development. Science China Earth Sciences, 67(9): 2937–2952, https://doi.org/10.1007/s11430-023-1335-8

1. Introduction

The Eocene-Oligocene transition (EOT) is one of the most important climatic transitions associated with global cooling during the Cenozoic, the onset of continental Antarctic glaciation and massive global sea-level drop (Zachos et al., 2001; Coxall et al., 2005; Pagani et al., 2011; Westerhold et al., 2020; Hutchinson et al., 2021). Introduced by Coxall and Pearson (2007) as a "phase of accelerated climate and biotic change", the EOT began before the Eocene-Oligocene boundary (33.9 Ma; Cohen et al., 2013) and lasted about 790 ka. Hutchinson et al. (2021) proposed a revised and updated the EOT timeframe. Thereafter, the base of the EOT

* Corresponding authors: Lutz KUNZMANN (lutz.kunzmann@senckenberg.de), Tao SU (sutao@cdut.edu.cn)

(hereafter called onset) was fixed by the tropical marine nannofossil extinction event at about 34.44 Ma. The top of the EOT (hereafter called offset) was fixed by a marked increase of $\delta^{18}O$ at about 33.65 Ma. It is proposed that the onset of the EOT is mainly associated with a pronounced cooling of ocean water, while the offset is primarily represented by a massive ice growth accompanied by a drop in sea level (Hutchinson et al., 2021). The latter caused significant paleogeographic changes in Eurasia, which was a major factor in the evolutionary step in the history of mammals called "Grand Coupure" (e.g., Hooker et al., 2004). The same paleogeographic changes might be the main reason for the presence of floristic migration routes across Eurasia in the early Oligocene (e.g., Akhmetiev et al., 2009). The decline of global atmospheric CO_2 (Beerling and Royer, 2011; Sheldon et al., 2012; Anagnostou et al., 2016; Elsworth et al., 2017), strengthening of changes in the Antarctic circumpolar current, opening of the Southern Ocean gateways (Tasman Seaway and Drake Passage) and orbital variations (Egan et al., 2013; Scher et al., 2015; Coxall et al., 2018; Tardif et al., 2021) may be driving factors of that climate transition (Coxall and Pearson, 2007). The EOT has been extensively studied and described from marine and terrestrial sediments (Zachos et al., 1996; Liu et al., 2009; Pearson et al., 2009; Coxall et al., 2018; Wade et al., 2020; Toumoulin et al., 2022). However, the magnitude and impact of regional climate change on paleoecosystems during this transition showed considerable variation, which influenced by factors such as tectonic activity and paleogeographic configurations (Chamberlain et al., 2012; Hren et al., 2013; Kocsis et al., 2014; Kargaranbafghi and Neubauer, 2018; Ding et al., 2022; Xie et al., 2022; Zheng et al., 2022). Terrestrial records show a rather heterogeneous response of fauna and vegetation to the global cooling (Kocsis et al., 2014; Pound and Salzmann, 2017). Indeed, while climate-related vegetation changes have been reported from many regions, certain locations show little to no discernible impact of global developments on regional and local climate and flora (Herman et al., 2017; Pound and Salzmann, 2017; Tosal et al., 2018).

For example, due to the growth of the Tibetan Plateau, a remarkable transition from dry to wet climate before the EOT was reported from the southeastern margin (Sorrel et al., 2017; Fang et al., 2021; Zheng et al., 2022). But, the onset of widespread aridification before the EOT was inferred in the Xining Basin which is located at the northeastern margin of the Tibetan Plateau (Dupont-Nivet et al., 2007, 2008; Barbolini et al., 2020). Therefore, more studies are needed to reveal the detailed mechanisms of terrestrial ecosystem responding to global changes during the EOT (Page et al., 2019).

The present study aims to describe changes in regional vegetation during the EOT in two geographically distant regions within Eurasia. These two regions provide successions of fossil floras from the Priabonian to the Rupelian that also cover the vegetation history before and after the EOT (Figure 1). In the first region, namely the southeastern margin of the Tibetan Plateau, which was strongly influenced by tectonic activities in the Cenozoic, a significant north-south elevational gradient was already established before the early Oligocene (Hoke, 2018; Su et al., 2019; Xiong et al., 2020; Wu et al., 2022). Modern plant diversity in that region had already occurred before the EOT (Su et al., 2019). In contrast, selected sites from the mid-latitudinal Europe were located in the lowland coastal plains of the palaeo-North Sea and in the nearby low-elevation volcanic-shaped hinterlands (Kvaček and Teodoridis, 2011; Standke et al., 2010; Kunzmann, 2012; Kunzmann and Walther, 2012). These sites are mostly affected by global sea level and temperature change, and relatively less affected by regional geological processes (Kvaček et al., 2014; Kunzmann et al., 2019). These two regions in Eurasia responded to global EOT processed independently and represent the regional histories of a lower latitude high-altitude montane zone and a mid-latitude low-altitude coastal zone. Furthermore, European Paleogene floras were similar to modern broad-leaved evergreen forests and mixed mesophytic forest from East and Southeast Asia (Teodoridis et al., 2012) making the present comparison feasible and plausible.

2. Materials and methods

2.1 Materials

Four assemblages of macrofossils from three localities were selected from the southeastern margin of the Tibetan Plateau. The formations at these sites were considered to be of Miocene in age based on regional lithostratigraphic comparison and various fossils (Writing Group of Cenozoic Plant of China, 1978). In recent years, the age of the three sites has been revised using radiometric dating, and all have been shown to be of Paleogene in age (Gourbet et al., 2017; Linnemann et al., 2018; Su et al., 2019). The fossil-bearing section at Lühe is composed of mudstone with several coaly layers and volcanic ash, the estimated age of the flora around 33±1 Ma (Linnemann et al., 2018). The regional vegetation reconstructed from pollen record and macrofossils indicates a deciduous broad-leaved forest mixed with evergreen broad-leaved elements (Tang et al., 2020; Wu et al., 2022). The age range of the Markam-1 site (upper Lawula Formation, 33.4±0.5 Ma) is associated with the EOT offset, while the estimated age of the Markam-3 site (lower Lawula Formation, 34.6±0.8 Ma) is associated with the EOT onset (Su et al., 2019). A recent study using a different isotope system for dating suggested that the Lawula Formation could be middle to the late Eocene in age (Zhao et al., 2023). The age dis-

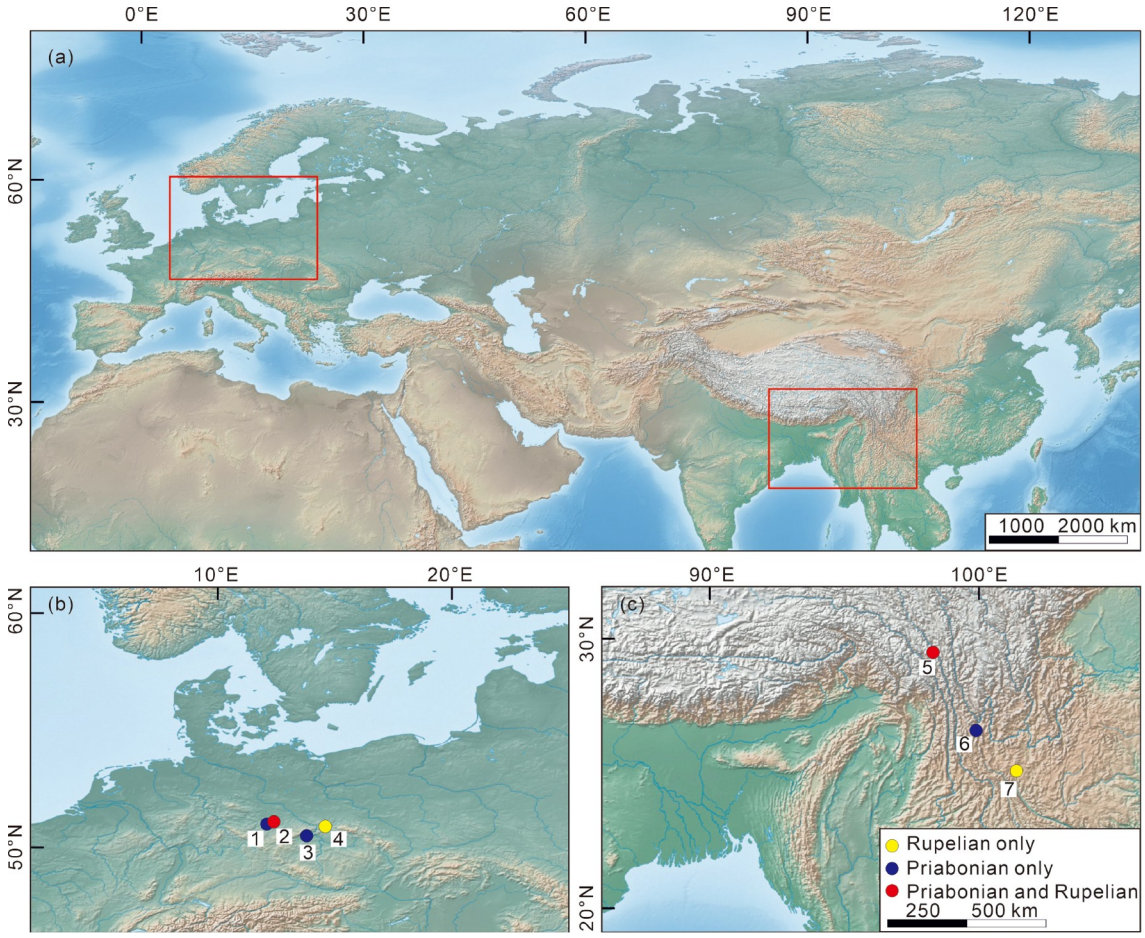

Figure 1 Locations of selected fossil sites. (a) Map of the study regions; the red rectangles refer to the mid-latitudinal Europe and the southeastern margin of the Tibetan Plateau, respectively; (b) enlargement of study areas in the mid-latitudinal Europe; (c) enlargement of study areas in the southeastern margin of the Tibetan Plateau. 1, Profen-Süd 3u; 2, Haselbach; 3, Kučlín; 4, Seifhennersdorf; 5, Markam; 6, Jianchuan; 7, Lühe.

crepancy between the two studies may be inherent in the dating methods. Herein, we followed the age concept of Su et al. (2019) whose results provided the details of the background data for our fossils. The plant assemblage from the late Eocene layer was dominated by Fagaceae and Betulaceae, but the dominate families changed to Rosaceae and Salicaceae in the early Oligocene (Deng et al., 2020). Cenozoic sedimentary rocks in the Jianchuan Basin consist of six formations, the coal-bearing Shuanghe Formation (35.9±0.9 Ma) yielding abundant plant fossils and providing a pre-EOT assemblage (Gourbet et al., 2017). Macrofossils indicated that the flora of Shuanghe was dominated by Fagaceae and Lauraceae, and the paleovegetation was a subtropical broad-leaved evergreen forest (Writing Group of Cenozoic Plant of China, 1978; Ge and Li, 1999) (Appendix Table S1, https://link.springer.com). Palynological records revealed more ferns and deciduous broadleaved components compared to the macrofossil assemblage (Wu et al., 2018).

Five fossil assemblages from four localities were selected to represent the vegetation history of the mid-latitudinal Europe. The Seifhennersdorf site is clearly younger than the EOT (Bellon et al., 1998), while the Haselbach HC assemblage is assumed to represent a time shortly after the EOT as a so-called "post Grand Coupure" flora (Akhmetiev et al., 2009). Three assemblages (Profen-Süd 3u, Kučlín, and Haselbach 2-3mi) are older than the EOT (Teodoridis and Kvaček, 2015; Moraweck et al., 2019). Kučlín, located in North Bohemia, Czech Republic, represents a subtropical zonal vegetation of a volcanic-shaped hinterland (Kvaček and Teodoridis, 2011), while the eastern German Seifhennersdorf assemblage represents a warm-temperate mixture of evergreen and deciduous vegetation from the same hinterland (Walther and Kvaček, 2007; Müller et al., 2023). Profen-Süd 3u and two Haselbach assemblages from the central German Weisselster area in the Leipzig Embayment mostly show an intrazonal aspect of coastal lowland riparian vegetation (Moraweck et al., 2015; Teodoridis and Kvaček, 2015; Kunzmann et al., 2019; Moraweck et al., 2019). For Profen-Süd 3u and Haselbach 2-3mi broad-leaved evergreen subtropical forests have been described (Mai and Walther, 2000). These assemblages originate from the Bruckdorf Member of the Borna Formation (Standke et al., 2010). The

Haselbach HC assemblage originates from the Gröbers Member of the Böhlen Formation (Standke et al., 2010) and is derived from a warm-temperate mixed mesophytic (evergreen/deciduous) forest (Kunzmann and Walther, 2007; Kunzmann and Walther, 2012) (Appendix Table S2). Comprehensive palynological data indicating the evolutionary history of the regional vegetation in central and east Germany are available (Krutzsch, 2011). In general, the palynological floras are assembled to complexes referring to an elaborated biostratigraphic spore-pollen zonation for this area. Krutzsch (2011) stated that the general vegetation history observed from palynological assemblages coincides with the results from the macrofloristic assemblages. The early-middle Priabonian Paleogene Spore-Pollen zone 18 corresponds to the subtropical evergreen broadleaved forest and the zone 20 A marks the earliest Oligocene with temperate mixed deciduous evergreen forest (Krutzsch, 2011). Zone 19, referred to late Priabonian age, is insufficiently known to date (Krutzsch, 2011). However, there are no compilations of microfloras available for the specific macrofloristic sites treated herein.

2.2 Methods

Since the study period covers a relatively long timeframe, taxonomic classification at the genus level is more suitable for studying the diversity of fossil floras (Cleal et al., 2021). Lists of fossil taxa (Appendix Table S1 and S2) of the fossil assemblages were compiled from the most recent publications (Table 1). Gymnosperm taxa are arranged according to the system proposed by Christenhusz et al. (2011) and the angiosperm classification follows the classification of the Angiosperm Phylogeny Group (APG) IV (APG, 2016).

The Integrated Plant Record (IPR) vegetation analysis, a semi-quantitative method for evaluating the main zonal vegetation types based on the plant fossil record, was applied (Kova-Eder and Kvaček, 2007; Teodoridis et al., 2011a). According to the IPR, the zonal and azonal plant elements are assigned to thirteen taxonomic-physiognomic groups, including the conifer component (CONIFER), the broad-leaved evergreen component (BLE), the broad-leaved deciduous component (BLD), the sclerophyllous component (SCL), the legume-like component (LEG), the zonal palm component (ZONPALM), the arborescent fern component (ARBFERN), the dry herbaceous component (DRY HERB), the mesophytic herbaceous component (MESO HERB), the azonal woody component (AZW), the azonal non-woody component (AZNW), the aquatic component (AQUA), and the elements with uncertain taxonomic-physiognomic affinity (PROBLEMATIC TAXA). Every taxon is assigned to the above components based on the fossil record and their closest living relatives. If a taxon is doubtfully assigned to one component, it is given a subdivided value in the respective components.

Based on the percentage of each group in a given fossil assemblage, IPR distinguishes six types of vegetation, namely broad-leaved deciduous forests (BLDF), mixed mesophytic forests (MMF), broad-leaved evergreen forests (BLEF), subhumid sclerophyllous forests (ShSF), xeric open woodlands (open woodland), and xeric grasslands or steppe (xeric grassland). In addition, ecotones between BLEF and MMF, and ecotones between BLDF and MMF were additionally defined (Teodoridis et al., 2011a, 2011b).

Taxonomic Similarity Drudges and Result-Mixes Drudges (Teodoridis et al., 2020) were applied to statistically determine close modern vegetation proxies for the selected fossil plant assemblages. As there is insufficient evidence of zonal herbs at the sites, only Drudge 1 could be applied (Teodoridis et al., 2020). The IPR results for Haselbach HC, Seifhennersdorf, Profen-Süd 3u, Haselbach 2-3mi, and Kučlín, have already been published by Teodoridis and Kvaček (2015). Although the Markam and Lühe score sheets are

Table 1 Selected the late Eocene and the early Oligocene study sites and assemblages

Epoch	Region	Site/assemblage	Age range (Ma)	Dating methods	Depositional environment	Reference
Early Oligocene	The mid-latitudinal Europe	Seifhennersdorf	30.7±0.7	K-Ar	Fresh water lake and swamp	Walther and Kvaček, 2007
		Haselbach HC	Unknown	Biostratigraphy	Riparian coastal plain	Kunzmann and Walther, 2012
	The southeastern margin of the Tibetan Plateau	Lühe	33±1/32±1	U-Pb	Fresh water lake	Linnemann et al., 2018
		Markam-1	33.4±0.5	$^{40}Ar/^{39}Ar$	Floodplain	Su et al., 2019
Late Eocene	The mid-latitudinal Europe	Profen-Süd 3u	35.8–35.4	Biostratigraphy	Riparian coastal plain	Moraweck et al., 2019
		Haselbach 2-3mi	36.7–36.4	Biostratigraphy	Riparian coastal plain	Moraweck et al., 2019
		Kučlín	38.3±0.9	Stratigraphical comparing	Fresh water lake	Kvaček and Teodoridis, 2011
	The southeastern margin of the Tibetan Plateau	Markam-3	34.6±0.8	$^{40}Ar/^{39}Ar$	Fresh water lake	Su et al., 2019
		Jianchuan	~35.9±0.9	U-Pb	Swamp	Gourbet et al., 2017

already included in the online database (www.iprdatabase.eu), the ages of these two sites have been updated and more fossil species have been reported from assemblages in recent years (Su et al., 2019; Deng et al., 2020; Wu et al., 2022). Therefore, new analyses are conducted for these two sites. The floristic assemblage of Jianchuan was analyzed for the first time (Appendix Table S3).

Leaf architectural characters show plant adaptation to environmental conditions (Sack and Scoffoni, 2013; McElwain et al., 2016; Li et al., 2022). Trait Combination Type (TCT) approach for fossil dicot leaves (Roth-Nebelsick et al., 2017), a semi-quantitative tool for describing the morphological "fingerprints" of entire leaf assemblages, was used to characterize the basic leaf physiognomic variability of fossil assemblages. Roth-Nebelsick et al. (2017) distinguished 16 Trait Combination Types (TCT) based on the combination of four-leaf architectural character sets. These sets are as follows: leaf lobed or unlobed, leaf margin toothed or untoothed, primary vein pattern pinnate or palmate, and secondary venation looped or non-looped.

The TCT results of the Kučlín and Seifhennersdorf assemblages were taken from Roth-Nebelsick et al. (2017). The TCT results of the Profen-Süd LC assemblage (Kunzmann et al., 2019) are used as a substitute for the Profen-Süd 3u assemblage. Both assemblages come from two close locations in the same lithostratigraphic unit. The substitution was necessary because the fragmented preservation of the fossil leaves in the Profen-Süd 3u assemblage prevents the application of the TCT approach. Accordingly, the Haselbach HC assemblage was replaced by unpublished assemblage data from the Schleenhain HC sampling site that comes from the same lithostratigraphic layer. For the Markam and Lühe assemblages from the southeastern margin of the Tibetan Plateau, representative subsamples of 10% of the leaves of the entire material were randomly selected. Due to the small number of leaf specimens (30 pieces) in the Jianchuan assemblage, all specimens were included in the analysis.

Paleoclimate parameters derived from the Climate-Leaf Analysis Multivariate Program (CLAMP) for the two regions have been published (Moraweck et al., 2019; Su et al., 2019; Wu et al., 2022). We compiled the published paleoclimate parameters and calculated the mean annual temperature range (MATR) value. Because at least 20 leaf morphotypes are required from a fossil assemblage to reveal reliable results. Therefore, the method is not applicable to the Profen-Süd 3u and Jianchuan assemblages. For Profen-Süd 3u, the values for the nearby Schleenhain 3u assemblage (same lithostratigraphic layer) published by Moraweck et al. (2019) are used. Regarding the TCT analysis, the CLAMP values of Schleenhain HC by Moraweck et al. (2019) are used as a substitute for the Haselbach HC assemblage. In total, 11 climate variables are calculated by CLAMP, from which the six most important variables are selected, namely mean annual temperature (MAT), warm month mean temperature (WMMT), cold month mean temperature (CMMT), mean growing season precipitation (GSP), precipitation in the three consecutive wettest months (3-WET), and precipitation in the three consecutive driest months (3-DRY). The WMMT value minus the CMMT value is used to estimate the MATR.

3. Results

3.1 Taxonomic diversity

16 families and 32 (fossil-)genera are reported from the late Eocene floras on the southeastern margin of the Tibetan Plateau (Appendix Table S1). Lauraceae, Rosacaeae, and Fagaceae are the most diverse broad-leaved components, i.e., each family is recorded with four (fossil-)genera (Figure 2). In the early Oligocene, diversity increased to 21 families and 43 (fossil-)genera. Rosacaeae and Betulaceae diversity increased to five and four genera in the early Oligocene, respectively, but Lauraceae diversity decreased from four to two (fossil-)genera. Fagaceae diversity remained stable with four genera, but the evergreen genus *Lithocarpus* disappeared and the deciduous genus *Castanea* appeared (Figure 2).

Taxonomic diversity in the mid-latitudinal Europe was generally about twice as high as in the southeastern margin of the Tibetan Plateau. However, the region experienced a slight decline in plant diversity across the EOT (Figure 2), from 55 families and 91 (fossil-)genera in the late Eocene to 50 families and 87 (fossil-)genera in the early Oligocene (Appendix Table S2). Some families that are recorded with only one or two genera such as Araceae, Rutaceae, and Rhamnaceae disappeared after the EOT. The diversity within some evergreen families such as Theaceae, was also reduced (Appendix Table S2). Lauraceae and Malvaceae are the most diverse families in the mid-latitudinal Europe in the late Eocene, each with five (fossil-)genera. The diversity of both families shows a slight decrease in the early Oligocene. At the same time, Rosaceae diversity increased notably from one genus to five genera. Nyssaceae and Betulaceae, not recorded from the late Eocene, are abundant with four genera each in the early Oligocene.

3.2 Abundance of evergreen components

Late Eocene floras show a higher percentage of BLE elements than early Oligocene floras in both regions (Figure 3). The coastal lowland floras of Haselbach 2-3mi and Profen-Süd 3u accounted for more than 75% of the BLE elements. However, BLE elements in the approximately coeval hinterland flora of Kučlín accounted for 40.7%, which is less

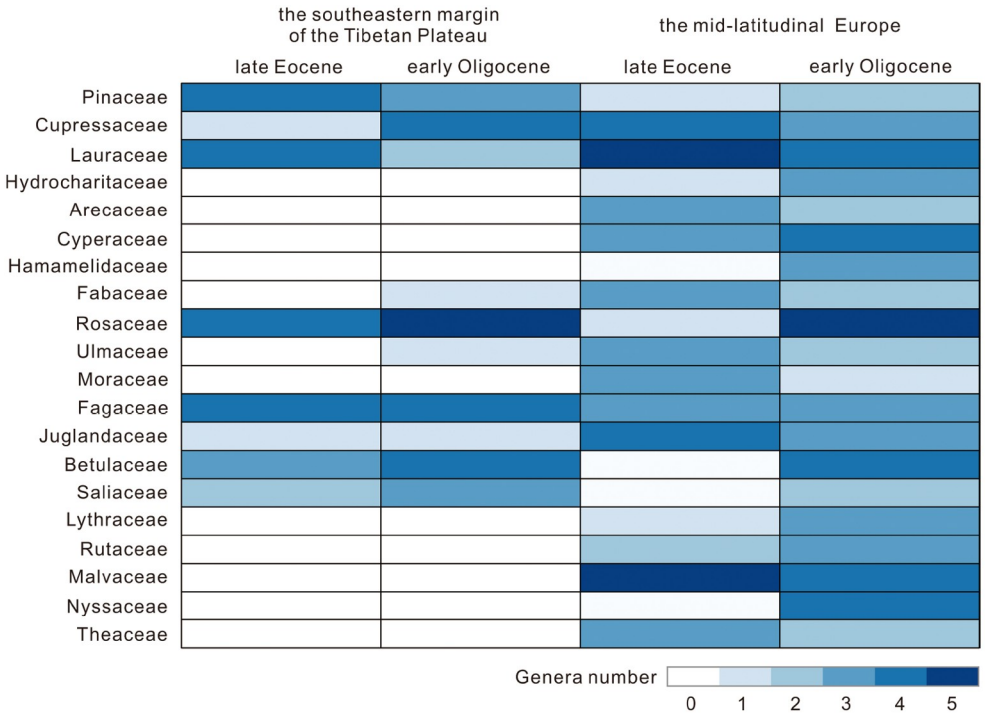

Figure 2 Number of (fossil-)genera of selected dominant families in fossil floras from the southeastern margin of the Tibetan Plateau and the mid-latitudinal Europe. For detailed information on (fossil-)genera and (fossil-)species, see Appendix Table S1 and S2.

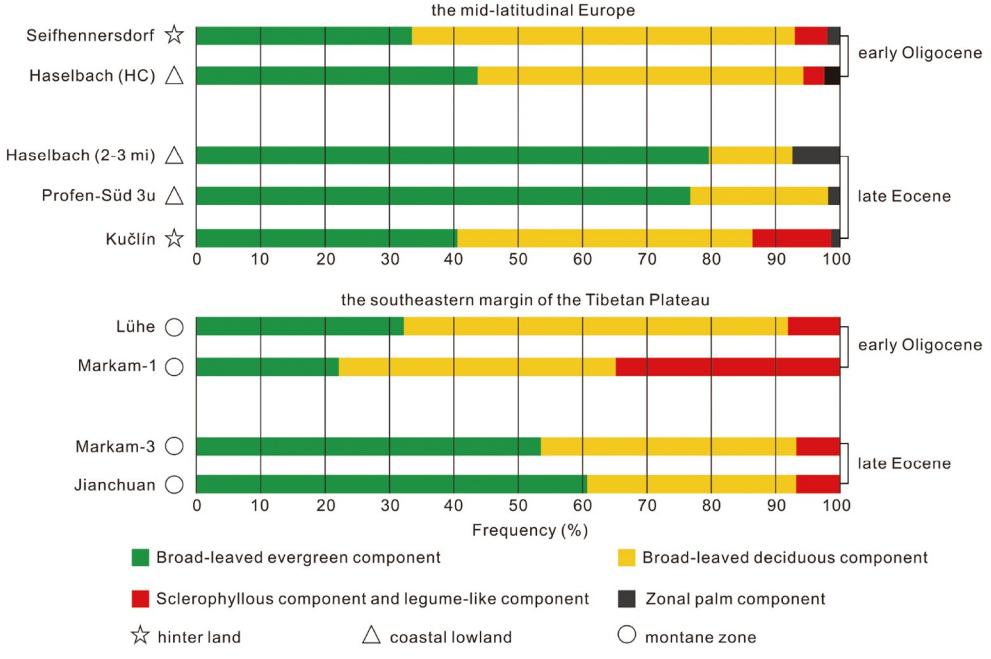

Figure 3 Percentages of zonal woody taxonomic-physiognomic components.

than in Jianchuan and Markam-3. ZONPALM has been reported from all assemblages in the mid-latitudinal Europe, while no palms have been recorded in assemblages from the southeastern margin of the Tibetan Plateau. The early Oligocene Markam-1 flora shows a high percentage of SCL and LEG and the lowest percentage of BLE elements. Based on the relative percentages of zonal woody components, all the late Eocene floras represent BLEF in this study. The flora of the early Oligocene Haselbach HC site is also BLEF, but the composition of the Seifhennersdorf flora is similar to both BLEF and MMF (ecotone). The southeastern margin of the Tibetan Plateau experienced a more significant change with

two early Oligocene assemblages interpreted as ecotone between the BLD and MMF and xeric open woodlands, respectively (Table 2).

The most similar extant vegetation units inferred by the Similarity Drudge 1 tool are located in East Asia (Table 2). Vegetation type inferred by similarity drudge and floristic composition are different in some assemblages, such as Haselbach HC, Lühe, Kučlín, and Markam-3. Both similarity drudge and floristic composition show a change in vegetation type at the EOT.

3.3 TCT frequency patterns

In all locations, the proportions of unlobed leaves are much higher than those of lobed leaves. TCT "P" is the only lobed leaf type at Markam-3, Lühe, and Seifhennersdorf (Figures 4 and 5). Kučlín differs in that it has four lobed types (TCT "I", "J", "O", and "P") but only accounted for 0.2% respectively. In all assemblages, except Kučlín, only one (Seifhennersdorf, Markam, Lühe, Jianchuan) or two (Schleenhain HC, Profen-Süd LC) TCTs predominate, together accounting for 65% or more of the TCT diversity for the assemblage. In Kučlín, TCTs "A", "B", "C", "E" and "F" are almost equally represented (Figure 6). The diversity of TCT ranges from three TCTs for Jianchuan to 12 TCTs for Kučlín (Figures 6 and 7). Riparian and floodplain assemblages dominated by intrazonal elements have lower TCT diversity (three or four TCTs) than assemblages from fresh water lake environments dominated by zonal elements. The latter reveal more than six TCTs (Seifhennersdorf, Lühe, Kučlín). The floras with the most diverse leaf architectural types are the Seifhennersdorf and Kučlín assemblages from the volcanic-shaped hinterland sites with eight and 12 TCTs, respectively.

Predominant TCTs often differ between the late Eocene and the early Oligocene assemblages. TCTs "F" (unlobed, toothed margin, pinnate 1° venation and non-looped secondaries) and "E" (unlobed, toothed margin, pinnate 1° venation and looped secondaries) dominate in all assemblages of the early Oligocene and in the late Eocene Markam-3. In the late Eocene Profen-Süd LC and Jianchuan assemblages, TCTs "A" and "B" (unlobed, entire-margined leaves with pinnate 1° venation) account for 85.2% and 72% of the total TCT diversities, respectively. The proportion of unlobed entire-margined leaves (TCTs "A"–"D") decreased substantially from the late Eocene to the early Oligocene. In contrast, the stratigraphy-related patterns for unlobed, toothed leaves (TCTs "E"–"H") differ and do not indicate a general increase from the late Eocene to the early Oligocene because TCTs "E" and "F" are already abundant in the Kučlín assemblage. Among the lobed leaf types, TCT "P" increased substantially from the late Eocene to the early Oligocene.

3.4 Paleoclimate

A comparison of the published climate parameters leads to the following data. The MAT for the late Eocene sites is higher than that from the early Oligocene (Table 3) in both studied regions. At the Markam site, MAT decreased from 17.8±2.3°C to 16.4±2.3°C. The decrease at the Schleenhain site was more pronounced, from 19.7±2.1°C to 14.2±1.3°C. The WMMT for the two Markam sites (28.0±2.8°C) remained unchanged from the late Eocene to the early Oligocene and is similar to the value for the early Oligocene Lühe site (27.2±2.8°C). The WMMT decreased slightly from the late Eocene to the early Oligocene in the mid-latitudinal Europe. On the contrary, this study region has experienced a dramatic change in CMMT. The CMMT for the Haselbach 2-

Table 2 Similarity Drudge 1 results for study sites[a)]

Sites	Vegetation code	Modern vegetation	Total difference	Vegetation type	
				Similarity drudge	Floristic composition
Haselbach HC	China 03	Mount Emei	72.2	MMF	BLEF
Seifhennersdorf	China 67	Eastern Guizhou	60.3	BLDF	MMF/BLEF
Markam-1	China 13	Meri Snow Mountain	42.5	ShSF	Open woodlands
Lühe	China 67	Eastern Guizhou	57.6	BLDF	Ecotone
Profen-Süd 3u	China 22	Longqi Mountain	82.1	BLEF	BLEF
Haselbach 2-3mi	Japan 11	Yamakushima Island	71.6	BLEF	BLEF
Kučlín	China 03	Mount Emei	95.6	MMF	BLEF
Markam-3	China 03	Mount Emei	47.7	MMF	BLEF
Jianchuan	China 36	Guizhou	42.8	BLEF	BLEF

a) Only the best-fitted results for each site were presented. MMF, mixed mesophytic forests; BLDF, broad-leaved deciduous forests; BLEF, broad-leaved evergreen forests; ShSF, subhumid sclerophyllous forests; Open woodland, xeric open woodlands.

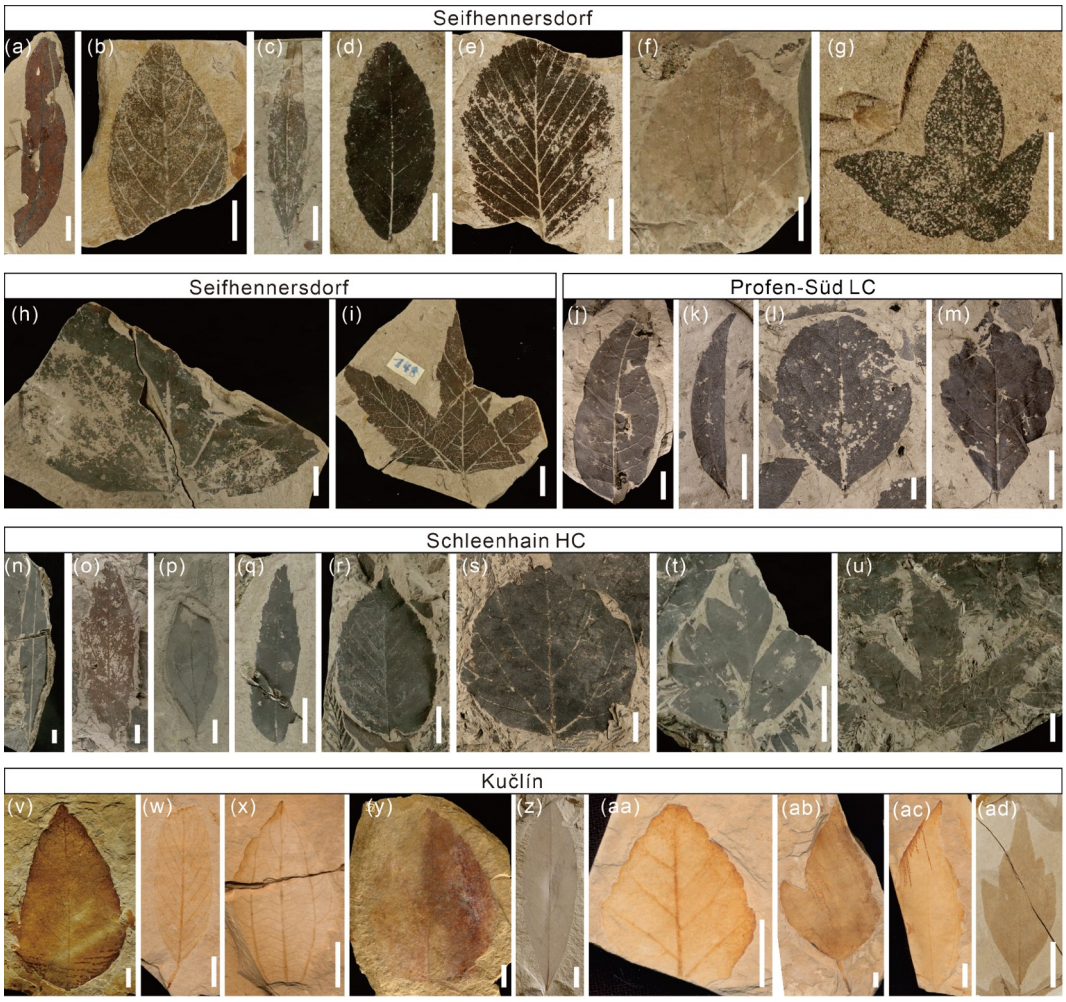

Figure 4 Selected taxa of the mid-latitudinal Europe and attribution to Trait Combination Types (TCTs) sensu Roth-Nebelsick et al. (2017). (a) *Lauraophyllum acutimontanum* (TCT "A"); (b) *Diospyros* sp. (TCT "B"); (c) *Daphnogene cinnamomifolia* (TCT "C"); (d) *Rosa lignitum* (TCT "E"); (e) *Betula alboides* (TCT "F"); (f) *Cercidiphyllym crenatum* (TCT "H"); (g) *Acer pseudomonspessulanum* (TCT "K"); (h) *Tilia gigantea* (TCT "L"); (i) *Acer angustilobum* (TCT "P"); (j) *Dicotylophyllum arcinerve* (TCT "A"); (k) *Laurophyllum* sp. (TCT "B"); (l) *Parasteinhauera fischkandelii* (TCT "E"); (m) *Sloanea nimrodi* (TCT "F"); (n) *Laurophyllum pseudoprinceps* (TCT "A"); (o) *Dicotylophyllum* sp. (TCT "B"); (p) *Daphnogene cinnamomifolia* (TCT "C"); (q) *Platanus neptuni* (TCT "E"); (r) *Carpinus grandis* (TCT "F"); (s) *Populusgermamica* (TCT "H"); (t) *Ampelopsis hibschii* (TCT "J"); (u) *Acer haselbachense* (TCT "P"); (v) *Byttneriopsis* sp. (TCT "A"); (w) *Leguminosites* sp. (TCT "B"); (x) *Daphnogene* sp. (TCT "C"); (y) *Ampelopsis* sp. (TCT "D"); (z) *Platanus neptuni* (TCT "E"); (aa) *Sloanea* sp. (TCT "F"); (ab) *Ziziphus bilinica* (TCT "H"); (ac) *Ampelopsis* sp. (TCT "J"); (ad) *Dicotylophyllum* sp. (TCT "O" or "P").

3mi site is 10.8±3.4°C in the late Eocene and 3.6±2.6°C in the early Oligocene site Schleenhain HC (substitute site for Haselbach HC). In the hinterland, the CMMT for the late Eocene Kučlín site is 8.1±2.6°C, but the value for the early Oligocene Seifhennersdorf is substantially lower (−1.6±2.6°C). MATR increased from the late Eocene to the early Oligocene in all assemblages. In the late Eocene, the average MATR was 17°C, while the value increased to 24°C in the early Oligocene. The MATR change of Markam assemble is 1.6°C, which is lower than for other assembles. GSP values for sites on the southeastern margin of the Tibetan Plateau and in the mid-latitudinal Europe decreased from the late Eocene to the early Oligocene. In the late Eocene, the mean GSP for the four sites is 1932 mm and it decreased to 1239 mm in the early Oligocene.

4. Discussion

4.1 Changes in vegetation types across the EOT

In most circumstances, mountainous terrain and low-latitude areas are important factors for higher biodiversity (Rahbek et al., 2019). Due to the Eocene greenhouse conditions, the climate in the mid-latitudinal Europe has been subtropical and sometimes even paratropical in the early Eocene (Kvaček and Teodoridis, 2011; Moraweck et al., 2015) that certainly triggered overall plant diversity. Moreover, we discuss diversity at the genus level but many divergence events within genera occurring in the southeast margin of the Tibetan Plateau happened during the Neogene (Yu et al., 2017; Chen et al., 2018). Therefore, the mid-latitudinal Europe showed higher generic plant diversity than the southeastern

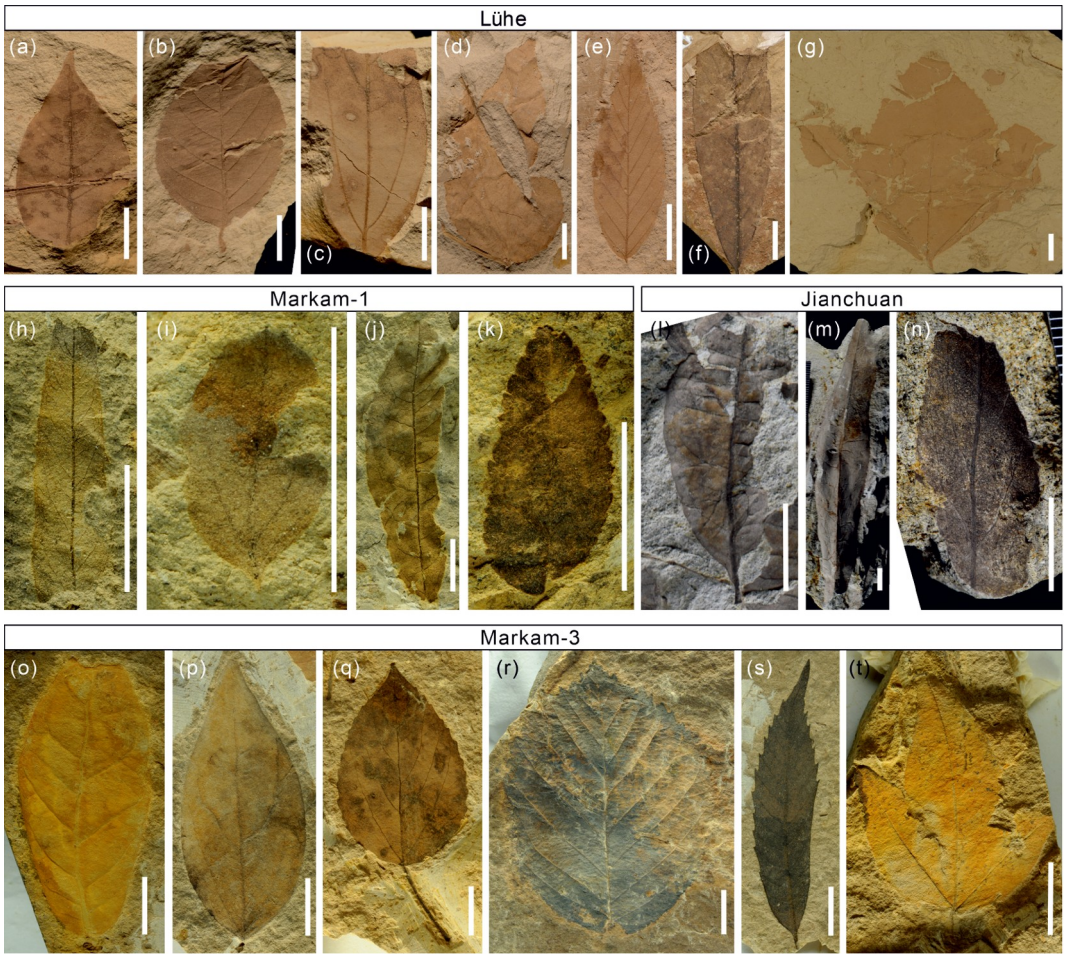

Figure 5 Selected taxa of the southeastern margin of the Tibetan Plateau and attribution to Trait Combination Types (TCTs) sensu Roth-Nebelsick et al. (2017). (a) Morphotype LH-1 (TCT "A"); (b) morphotype LH-2 (TCT "B"); (c) *Cinnamomum* sp. (TCT "C"); (d) *Idesia* sp. (TCT "E"); (e) *Carpinus* sp. (TCT "F"); (f) *Quercus* sp. (TCT "F"); (g) *Acer* sp., (TCT "P"). (h) *Salix* sp. (TCT "A"); (i) *Cotoneaster* sp. (TCT "C"); (j) *Spiraea* sp. (TCT "E"); (k) *Rosa* sp. (TCT "F"); (l) morphotype JC-1 (TCT "A"); (m) morphotype JC-2 (TCT "E"); (n) morphotype JC-3 (TCT "A"); (o) *Quercus* cf. *presenescens* (TCT "A"); (p) *Lindera* sp. (TCT "C"); (q) *Populus* sp. (TCT "E"); (r) *Betula* sp. (TCT "F"); (s) *Quercus tibetensis* (TCT "F"); (t) *Acer* sp. (TCT "P").

Table 3 Paleoclimate estimates derived using the Climate Leaf Analysis Multivariate Program (CLAMP)[a)]

Epoch	Site	MAT (°C)	WMMT (°C)	CMMT (°C)	MATR (°C)	GSP (mm)	3-WET (mm)	3-DRY (mm)	References
Early Oligocene	Seifhennersdorf	10.0±1.3	22.9±1.7	−1.6±2.6	24.5±2.6	849.4±497	559.2±239	140.4±104	Moraweck et al., 2019
	Schleenhain HC	14.2±1.3	25.0±1.7	3.6±2.6	21.4±2.6	654.5±497	445.7±239	76.4±104	Moraweck et al., 2019
	Lühe	14.9±2.3	27.2±2.8	1.8±3.6	25.4±3.6	1748.5±606	804.3±358	232.4±95	Wu et al., 2022
	Markam-1	16.4±2.3	28.0±2.8	3.2±3.6	24.8±3.6	1704.0±606	768.0±358	196.0±95	Su et al., 2019
Late Eocene	Schleenhain 3u	19.7±2.1	26.3±2.5	13.6±3.4	12.7±3.4	1902.5±317	917±229	172.0±59	Moraweck et al., 2019
	Haselbach 2-3 mi	17.9±2.1	25.5±2.5	10.8±3.4	14.7±3.4	2403.1±317	1226.6±229	187.7±59	Moraweck et al., 2019
	Kučlín	16.8±1.3	26.1±1.7	8.1±2.6	18.0±2.6	1267.0±497	638.0±239	142.0±104	Moraweck et al., 2019
	Markam-3	17.8±2.3	28.0±2.8	4.8±3.6	23.2±3.6	2157.0±606	957.0±358	313.0±95	Su et al., 2019

a) MAT, WMMT, CMMT, GSP, 3-WET, and 3-DRY were compiled from the listed references, while MATR values were calculated in this study. MAT, mean annual temperature; WMMT, warm month mean temperature; CMMT, cold month mean temperature; MATR, mean annual temperature range; GSP, mean growing season precipitation; 3-WET, precipitation during the three consecutive wettest months; X3- DRY, precipitation during the three consecutive driest months.

margin of the Tibetan Plateau, although preservation and taphonomic biases and the status of scientific processing of the fossil floras might have influenced the biodiversity data as well.

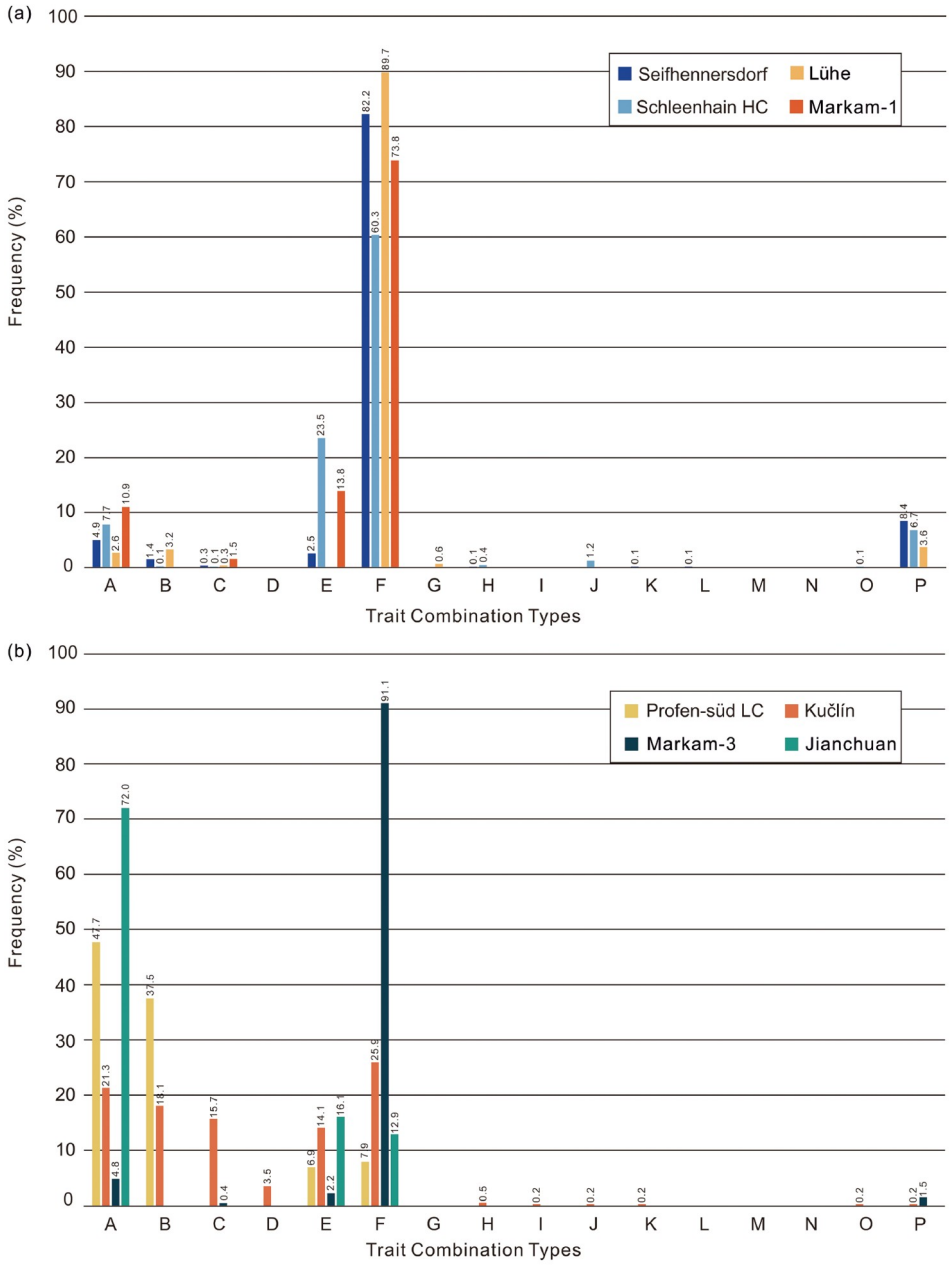

Figure 6 Results of TCT analysis for the early Oligocene assemblages (a) and late Eocene assemblages (b). Frequency values for Lühe, Schleenhain HC (replacement for Haselbach HC), Markam and Jianchuan are from this study; values for Seifhennersdorf are from Müller et al. (2023) and values for Kučlin and Profen-Süd LC (replacement for Profen-Süd 3u) are from Kunzmann et al. (2019).

Both in the southeastern margin of the Tibetan Plateau and in the mid-latitudinal Europe, paleovegetation responded to paleoclimate change across the EOT. Assemblages from the southeastern margin of the Tibetan Plateau show an increase in plant diversity, while the mid-latitudinal European assemblages show a slight decrease (Figure 2). In both regions, the diversity of temperate deciduous taxa (e.g., Betulaceae and Rosaceae) increased in number of genera, while the diversity of evergreen taxa (e.g., Lauraceae) decreased. The trend of reduced proportions of BLE elements and increased proportions of BLD elements across the EOT known from previous studies (e.g., Teodoridis and Kvaček, 2015) was again recognized in this study (Figure 3). It is expressed by a general change in the overall type of vegetation from BLEF in the late Eocene to BLDF or MMF in the early Oligocene (Table 2). This transition is more gradual than occurring as a single significant step in both regions as the ecotone between BLEF and MMF is reconstructed for several assemblages, e.g., Seifhennersdorf and Lühe. Nevertheless, it should be noted that between these two regions there is marked heterogeneity in taxonomic diversity and overall leaf architectural "fingerprints". The late Eocene and early Oligocene

floras of the mid-latitudinal Europe are compared with the modern BLEF of subtropical China and Japan, rather than with the modern floras of Europe and North America (Table 2). Genera endemic to East Asia such as *Cephalotaxus*, *Cercidiphyllum*, *Craigia*, *Fortunearia* and fossils-genera without close systematic connections with the present European flora such as *Eotrigonobalanus*, *Rhodomyrtophyllum* and *Daphnogene* were found (Moraweck et al., 2019).

BLE elements show the highest percentages of the predominantly intrazonal paleovegetation from the coastal lowland of the mid-latitudinal Europe in the late Eocene, and the proportion decreased towards the early Oligocene. However, this trend had already started in the hinterland in volcanic-shaped landscapes in the latest Eocene, as evidenced by the flora of Roudníky, Czech Republic (Kvaček et al., 2014). Thus, the relative decrease in BLE elements across the EOT is lower in the hinterland assemblages that mainly represent zonal paleovegetation. The paleoclimate of the mid-latitudinal Europe transformed from subtropical-humid to warm-temperate humid regimes (Kvaček et al., 2014), which resulted in the decline of subtropical evergreen plant species in favor of temperate deciduous elements that immigrated mainly from Asia to the mid-latitudinal Europe after the closure of the central Asian Turgai Strait (Akhmetiev et al., 2009). Due to the lack of a coeval flora for Roudníky directly in the coastal lowland plains, it remains unknown whether the immigration of temperate elements reached the coastal plains in the latest Eocene. Nonetheless, it seems that the immigration of temperate elements into the hinterland vegetation had already started before the Grand Coupure in the mid-latitudinal Europe and that the beginning probably coincides with the onset of the EOT ca. 34.44 Ma (Hutchinson et al., 2021). The Haselbach HC flora, the earliest Oligocene flora known so far from the coastal lowland, was previously interpreted as a post-Grand Coupure flora (Akhmetiev et al., 2009) meaning a post-EOT flora according to the concept of Hutchinson et al. (2021). However, according to the regional biostratigraphic concept, the Haselbach HC sediment bed contains the first occurrence of the palynomorph *Boehlensispollis hohlii* that marks the beginning of the Oligocene in central and eastern Germany (palynomoph zone 20) (Krutzsch, 2011). It means that the Haselbach HC flora could indeed be placed within the EOT but there is no better precise age estimate for evidence. All-in-all, the macrofloristic data implicate a beginning of vegetation change in the mid-latitudinal Europe from subtropical BLEF to warm-temperate MMF within the EOT and before the Grand Coupure. On the contrary, the flora of the southeastern margin of Tibetan Plateau is similar to the modern vegetation in the surrounding area since the late Eocene (Table 2). Most of the reported (fossil-)genera have their closest living relatives distributed in or near the region of fossil sites. The floristic modernization of this region before the early Oligocene (Su et al., 2019; Wu et al., 2022), numerous modern genera appeared in the Paleogene, including the constructive genera of modern evergreen broadleaved forests, such as *Quercus* sect. *Cyclobalanopsis*.

Regarding the northeastern Tibetan Plateau, steppe-desert has existed in the Xining Basin since at least Eocene (Barbolini et al., 2020). Significant decreased in abundance and diversity of the dominant Nitrariaceae-Ephedraceae shrubs while both abundance and diversity of conifer pollen significantly increased across the EOT (Dupont-Nivet et al., 2008; Barbolini et al., 2020). Although a high percentage of BLD elements appeared in the early Oligocene (30.8 Ma) of the Qaidam Basin in northeastern Tibetan Plateau (Song et al., 2020), the diversity of other species decreased (Wang et al., 2017; Song et al., 2020).

4.2 Changes to leaf architectural "fingerprints" across the EOT

Assemblages from lacustrine or swamp environments show more TCTs than assemblages from riparian or floodplain paleoenvironments (Figure 7). Kučlín and Seifhennersdorf, both representatives from lacustrine sedimentary paleoenvironments in the volcanic-shaped hinterland, show the most diverse distribution pattern ("fingerprint") of TCT. These TCT diversities correspond to high taxonomic diversities in the two assemblages (Figure 6). Although the Jianchuan assemblage also originates from a swamp environment, poor fossil preservation likely resulted in fewer taxa and TCTs identified.

The lobed and palmate veined leaves show greater leaf area and the lowest values for leaf mass per area in all TCTs which means a rapidly pay back the low investment put into them (Roth-Nebelsick et al., 2017). The increase in TCT "P" (Figure 6) may indicate an adaptation to increasing of temperature seasonality in the early Oligocene. Another remarkable change occurred in the leaf margin and secondary venation. The proportion of TCT "A" (untoothed, looped secondaries) decreased, while the proportion of TCT "F" (toothed, non-looped) increased simultaneously (Figure 6). Compared to toothed leaves with non-looped secondaries, entire-margined leaves with looped secondaries may indicate a leaf type that is better protected against water stress (Roth-Nebelsick et al., 2017). Thus, taxa with looped secondaries appear to be particularly common in modern subtropical/tropical evergreen vegetation, while the toothed non-looped leaf type is predominant in temperate vegetation (Walls, 2011). In modern flora, TCT "A" leaves are more common in evergreen species, while TCT "F" leaves are more common in deciduous species (Su et al., 2010; Royer et al., 2012; Li et al., 2016; Müller et al., 2023). The change in leaf architecture across the EOT recognized from our study assemblages corresponds with the decrease in BLE elements and the in-

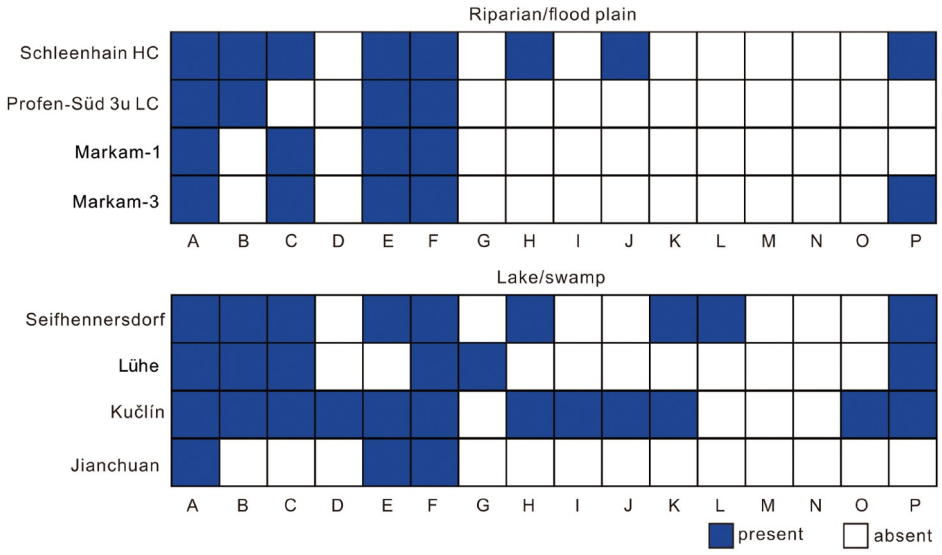

Figure 7 Differences in leaf architectural type diversity (TCT) in riparian/flood plain and lake/swamp sedimentary environments.

crease in BLD elements.

The two assemblages of the Markam site show a different adaptation strategy of leaf architecture across the EOT. The TCT "fingerprint" remains almost unchanged except for the disappearance of TCT "P" in the Markam-1 assemblage although the dominant families have changed. The late Eocene Markam-3 assemblage shows a high percentage of TCT "F" and a low percentage of TCT "A" which is more similar to that of the early Oligocene flora rather than to that of the late Eocene flora (Figure 6). As already mentioned above, the vegetation type of the Roudníky assemblage from the mid-latitudinal Europe also shows an already close relationship in leaf composition and architecture with the early Oligocene flora of that region (Kvaček et al., 2014).

In summary, the dominant leaf architectural types in the mid-latitudinal European assemblages change from TCT "A" to TCT "F" (Figure 6). This transition corresponds to a decrease in evergreen elements and an increase in temperate elements, as well as a transition from predominantly BLEF to predominantly MMF in this region. The history of the presence of specific leaf architectural types in the assemblages on the southeastern margin of the Tibetan Plateau is more complicated. The Jianchuan assemblage was dominated by TCT "A" (Figure 6) which is similar to contemporary sites in the mid-latitudinal Europe. However, TCT "F" dominated the Markam assemblages since the late Eocene and a distinct reduction in leaf size was observed between Markam-3 and Markam-1 assemblages (Su et al., 2019). Therefore, it can be assumed that the paleovegetation at the Markam site adapted to paleoenvironmental changes across the EOT through a change in leaf size rather than a change in leaf margin type and secondary venation type. This is because small leaves, which produce less wind-induced drag forces and require lower mechanical resistance, are more likely to be favored at higher altitudes (Pan et al., 2013). A strategy of changing leaf size could be the response to the rapidly rising landscape in this region.

4.3 Drivers of changes in floristic heterogeneity

GSP decreased across the EOT in both studied regions (Table 3). The GSP was reduced to 80% and rainfall seasonality increased in Markam (Su et al., 2019). Rainfall seasonality existed in the Lühe area during the early Oligocene but was not as significant as in present-days (Wu et al., 2022). However, the mid-latitudinal Europe showed a decrease in rainfall seasonality. The decrease of GSP in coastal low land was higher than that in the hinterland (Table 3). MAT decreased from the late Eocene to the early Oligocene in both studied regions (Table 3) as well, which is consistent with a global cooling trend. Pronounced cooling in winter leading to increased temperature seasonality has already been reported in parts of the Northern Hemisphere (Kvaček et al., 2014; Toumoulin et al., 2022). The increase in seasonality and most of the global heterogeneity in the MATR was caused by global sea-level decrease in the earliest Oligocene (Miller et al., 2008; Houben et al., 2012; Toumoulin et al., 2022). However, sea level rose in the mid-latitudinal Europe and reached its highest in the mid-early Oligocene (Kunzmann, 2012). Changes in MATR in this region are associated with decreases in CMMT (Table 3). Since the Eocene greenhouse conditions, the climate in the mid-latitudinal Europe has been subtropical and sometimes even paratropical (Moraweck et al., 2015). When the paleoclimate changed to a warm temperate climate, the mean annual temperature range increased (Kvaček et al., 2014).

In addition to the impact of global cooling, the southeastern margin of the Tibetan Plateau experienced dramatic regional geological processes. Southeastern Tibetan Plateau rapidly uplifted during the Eocene (Xiong et al., 2020; He et al., 2022) and reached high altitude at least since the early Oligocene (Hoke, 2018; Su et al., 2019; Wu et al., 2022; Zhou et al., 2023). The Markam Basin, located on the SE margin of the Tibetan Plateau, already reached ~3 km of paleoelevation in the latest Eocene (~34 Ma) and was close to its present height during the EOT (3.9 km) (Su et al., 2019). Therefore, the flora of Markam-3 hints at the pronounced immigration of temperate floristic elements before the EOT, which makes this flora already similar to early Oligocene flora.

However, CLAMP data indicate a rather large standard error, i.e., a range of 4.6°C of the MAT values. Calculating using the Coexistence Approach revealed less meaningful results than CLAMP, e.g., MAT of Markam-3 was 7.2–17.6°C and MAT of Markam-1 was 5.4–15.3°C (Deng et al., 2020). Thus, Coexistence Approach results cannot contribute to resolve the question why the temperature decline in the high-elevation area was seemingly low across EOT. However, based on this minor temperature decline the dominant leaf architectural types, i.e., TCT, remained the same at Markam, but leaves became smaller adapting to higher altitudes and a drier paleoenvironment (Scoffoni et al., 2011; Pan et al., 2013). On the contrary, the paleoelevation of the late Eocene Jianchuan flora (Shuanghe Formation) was slightly lower than the modern elevation range (Wu et al., 2018) and the MAT shows a warmer paleoclimate than today (Sun et al., 2011; Wu et al., 2018). In addition, the sedimentary faces of the Shuanghe Formation indicate semi-humid to humid paleoclimatic conditions (Sorrel et al., 2017; Zheng et al., 2022). The warm and humid paleoclimate and relatively lower paleoaltitude led to a higher percentage of BLE elements in the Jianchuan flora compared to the Markam-3 flora. In particular, the late Eocene Jianchuan assemblage was dominated by Lauraceae and Fagaceae (Writing Group of Cenozoic Plant of China, 1978) and untoothed leaf types.

Sea-level changes in the mid-latitudinal Europe and the uplift of the Tibetan Plateau have led to changes in paleovegetation and leaf architecture in these two regions. The degree of change is less pronounced in the hinterland compared to the coastal lowland plains. On the southeastern margin of the Tibetan Plateau, vegetation changes decreased with distance from the plateau. All these above reflects the complexity of factors that shape biodiversity in different regions around the world.

5. Conclusions

Paleogene floras in both the mid-latitudinal Europe and the southeastern margin of the Tibetan Plateau resembled modern evergreen broad-leaf forests in East Asia. While percentages of BLE elements decreased and general vegetation types changed in both the southeastern margin of the Tibetan Plateau and the mid-latitudinal Europe during the EOT. The simultaneous increase in the percentage of deciduous taxa, i.e., plants that form "low cost" leaves (economically called a fast return strategy), is interpreted as an adaptation to the increasing temperature seasonality towards the early Oligocene. Global cooling at the EOT led to a decrease in MAT and an increase in MATR at the southeastern margin of the Tibetan Plateau and in the mid-latitudinal Europe. Sea-level changes in the mid-latitudinal Europe and the uplift of the Tibetan Plateau have led to heterogeneous responses in paleovegetation and leaf architecture in these two regions.

Acknowledgements *The authors thank Weiyudong DENG and Christian MÜLLER for data collecting. We are also grateful to two reviewers for their comments. This work was supported by the National Key R&D Program of China (Grant No. 2022YFF0800800), the National Natural Science Foundation of China (Grant Nos. 42072024 & 42320104005), and the Sino-German (CSC-DAAD) Postdoc Scholarship Program (Grant No. 57607866).*

Conflict of interest The authors declare that they have no conflict of interest.

References

Akhmetiev M, Walther H, Kvaček Z. 2009. Paleogene floras of Eurasia bound to volcanic settings and palaeoclimatic events—Experience obtained from the Far East of Russia (Sikhote-Alin') and Central Europe (Bohemian Massif). Acta Musei Natl Pragae Ser B, 65: 61–129

Anagnostou E, John E H, Edgar K M, Foster G L, Ridgwell A, Inglis G N, Pancost R D, Lunt D J, Pearson P N. 2016. Changing atmospheric CO_2 concentration was the primary driver of early Cenozoic climate. Nature, 533: 380–384

Angiosperm Phylogeny Group. 2016. An update of the angiosperm phylogeny group classification for the orders and families of flowering plants: APG IV. Bot J Linn Soc, 181: 1–20

Barbolini N, Woutersen A, Dupont-Nivet G, Silvestro D, Tardif D, Coster P M C, Meijer N, Chang C, Zhang H X, Licht A, Rydin C, Koutsodendris A, Han F, Rohrmann A, Liu X J, Zhang Y, Donnadieu Y, Fluteau F, Ladant J B, Le Hir G, Hoorn C. 2020. Cenozoic evolution of the steppe-desert biome in Central Asia. Sci Adv, 6: eabb8227

Beerling D J, Royer D L. 2011. Convergent Cenozoic CO_2 history. Nat Geosci, 4: 418–420

Bellon H, Bůžek Č, Gaudant J, Kvaček Z, Walter H. 1998. The Českе Středohoří magmatic complex in Northern Bohemia ^{40}K-^{40}Ar ages for volcanism and biostratigraphy of the Cenozoic freshwater formations. Newsl Stratigr, 36: 77–103

Chamberlain C P, Mix H T, Mulch A, Hren M T, Kent-Corson M L, Davis S J, Horton T W, Graham S A. 2012. The Cenozoic climatic and topographic evolution of the western North American Cordillera. Am J Sci, 312: 213–262

Chen Y S, Deng T, Zhou Z, Sun H. 2018. Is the East Asian flora ancient or not? Natl Sci Rev, 5: 920–932

Christenhusz M J M, Reveal J L, Farjon A, Gardner M F, Mill R R, Chase M W. 2011. A new classification and linear sequence of extant gymnosperms. Phytotaxa, 19: 55–70

Cleal C, Pardoe H S, Berry C M, Cascales-Miñana B, Davis B A S, Diez J

B, Filipova-Marinova M V, Giesecke T, Hilton J, Ivanov D, Kustatscher E, Leroy S A G, McElwain J C, Opluštil S, Popa M E, Seyfullah L J, Stolle E, Thomas B A, Uhl D. 2021. Palaeobotanical experiences of plant diversity in deep time. 1: How well can we identify past plant diversity in the fossil record? Palaeogeogr Palaeoclimatol Palaeoecol, 576: 110481
Cohen K M, Finney S C, Gibbard P L, Fan J X. 2013. The ICS international chronostratigraphic chart. Episodes, 36: 199–204
Coxall H K, Pearson P N. 2007. The Eocene-Oligocene transition. In: Williams M, Haywood A M, Gregory F J, Schmidt, D N, eds. The Micropalaeontological Society, Special Publications, London: The Geological Society
Coxall H K, Wilson P A, Pälike H, Lear C H, Backman J. 2005. Rapid stepwise onset of Antarctic glaciation and deeper calcite compensation in the Pacific Ocean. Nature, 433: 53–57
Coxall H K, Huck C E, Huber M, Lear C H, Legarda-Lisarri A, O'Regan M, Sliwinska K K, van de Flierdt T, de Boer A M, Zachos J C, Backman J. 2018. Export of nutrient rich northern component water preceded early Oligocene Antarctic glaciation. Nat Geosci, 11: 190–196
Deng W Y D, Su T, Wappler T, Liu J, Li S F, Huang J, Tang H, Low S L, Wang T X, Xu H, Xu X T, Liu P, Zhou Z K. 2020. Sharp changes in plant diversity and plant-herbivore interactions during the Eocene-Oligocene transition on the southeastern Qinghai-Tibetan Plateau. Glob Planet Change, 194: 103293
Ding L, Kapp P, Cai F L, Garzione C N, Xiong Z Y, Wang H Q, Wang C. 2022. Timing and mechanisms of Tibetan Plateau uplift. Nat Rev Earth Environ, 3: 652–667
Dupont-Nivet G, Krijgsman W, Langereis C G, Abels H A, Dai S, Fang X M. 2007. Tibetan Plateau aridification linked to global cooling at the Eocene-Oligocene transition. Nature, 445: 635–638
Dupont-Nivet G, Hoorn C, Konert M. 2008. Tibetan uplift prior to the Eocene-Oligocene climate transition: Evidence from pollen analysis of the Xining Basin. Geology, 36: 987–990
Egan K E, Rickaby R E M, Hendry K R, Halliday A N. 2013. Opening the gateways for diatoms primes Earth for Antarctic glaciation. Earth Planet Sci Lett, 375: 34–43
Elsworth G, Galbraith E, Halverson G, Yang S. 2017. Enhanced weathering and CO_2 drawdown caused by latest Eocene strengthening of the Atlantic meridional overturning circulation. Nat Geosci, 10: 213–216
Fang X M, Yan M D, Zhang W L, Nie J S, Han W X, Wu F L, Song C H, Zhang T, Zan J B, Yang Y P. 2021. Paleogeography control of Indian monsoon intensification and expansion at 41 Ma. Sci Bull, 66: 2320–2328
Ge H R, Li D Y. 1999. Cenozoic Coal Bearing Basins and Coal Accumulation Law in Western Yunnan (in Chinese). Kunming: Yunnan Science and Technology Press. 52
Gourbet L, Leloup P H, Paquette J L, Sorrel P, Maheo G, Wang G C, Xu Y D, Cao K, Antoine P O, Eymard I, Wei L, Lu H J, Replumaz A, Chevalier M L, Zhang K X, Wu J, Shen T Y. 2017. Reappraisal of the Jianchuan Cenozoic basin stratigraphy and its implications on the SE Tibetan plateau evolution. Tectonophysics, 700-701: 162–179
He S L, Ding L, Xiong Z Y, Spicer R A, Farnsworth A, Valdes P J, Wang C, Cai F L, Wang H Q, Sun Y, Zeng D, Xie J, Yue Y H, Zhao C Y, Song P P, Wu C. 2022. A distinctive Eocene Asian monsoon and modern biodiversity resulted from the rise of eastern Tibet. Sci Bull, 67: 2245–2258
Herman A B, Spicer R A, Aleksandrova G N, Yang J, Kodrul T M, Maslova N P, Spicer T E V, Chen G, Jin J H. 2017. Eocene-early Oligocene climate and vegetation change in southern China: Evidence from the Maoming Basin. Palaeogeogr Palaeoclimatol Palaeoecol, 479: 126–137
Hoke G D. 2018. Geochronology transforms our view of how Tibet's southeast margin evolved. Geology, 46: 95–96
Hooker J J, Collinson M E, Sille N P. 2004. Eocene-Oligocene mammalian faunal turnover in the Hampshire Basin, UK: Calibration to the global time scale and the major cooling event. J Geol Soc London, 161: 161–172
Houben A J P, van Mourik C A, Montanari A, Coccioni R, Brinkhuis H. 2012. The Eocene-Oligocene transition: Changes in sea level, temperature or both? Palaeogeogr Palaeoclimatol Palaeoecol, 335-336: 75–83
Hren M T, Sheldon N D, Grimes S T, Collinson M E, Hooker J J, Bugler M, Lohmann K C. 2013. Terrestrial cooling in Northern Europe during the Eocene-Oligocene transition. Proc Natl Acad Sci USA, 110: 7562–7567
Hutchinson D K, Coxall H K, Lunt D J, Steinthorsdottir M, de Boer A M, Baatsen M, von der Heydt A, Huber M, Kennedy-Asser A T, Kunzmann L, Ladant J B, Lear C H, Moraweck K, Pearson P N, Piga E, Pound M J, Salzmann U, Scher H D, Sijp W P, Śliwińska K K, Wilson P A, Zhang Z S. 2021. The Eocene-Oligocene transition: A review of marine and terrestrial proxy data, models and model-data comparisons. Clim Past, 17: 269–315
Kargaranbafghi F, Neubauer F. 2018. Tectonic forcing to global cooling and aridification at the Eocene-Oligocene transition in the Iranian plateau. Glob Planet Change, 171: 248–254
Kocsis L, Ozsvart P, Becker D, Ziegler R, Scherler L, Codrea V. 2014. Orogeny forced terrestrial climate variation during the late Eocene-early Oligocene in Europe. Geology, 42: 727–730
Kova-Eder J, Kvaček Z. 2007. The integrated plant record(IPR)to reconstruct Neogene vegetation: The IPR-vegetation analysis. Acta Palaeobot, 47: 391–418
Krutzsch W. 2011. Stratigraphy and climate of the Palaeogene in the Central German estuary and related marine environment. Z Dtsch Ges Geowiss, 162: 19–46
Kunzmann L. 2012. Early Oligocene riparian and swamp forests with a mass occurrence of *Zingiberoideophyllum* (extinct zingiberales) from Saxony, central Germany. Palaios, 27: 765–778
Kunzmann L, Walther H. 2007. A noteworthy plant taphocoenosis from the Lower Oligocene Haselbach Member (Saxony, Germany) containing *Apocynophyllumneriifolium* Heer. Acta Palaeobot, 47: 145–161
Kunzmann L, Walther H. 2012. Early Oligocene plant taphocoenoses of the Haselbach megafloral complex and the reconstruction of palaeovegetation. Palaeobio Palaeoenv, 92: 295–307
Kunzmann L, Moraweck K, Müller C, Schröder I, Wappler T, Grein M, Roth-Nebelsick A. 2019. A Paleogene leaf flora (Profen, Sachsen-Anhalt, Germany) and its potentials for palaeoecological and palaeoclimate reconstructions. Flora, 254: 71–87
Kvaček Z, Teodoridis V. 2011. The Late Eocene flora of Kučlín near Bílina in North Bohemia revisited. Acta Musei Natl Pragae Ser B, 67: 83–144
Kvaček Z, Teodoridis V, Mach K, Přikryl T, Dvořák Z. 2014. Tracing the Eocene-Oligocene transition: A case study from North Bohemia. Bull Geosci, 89: 1411
Li Y, Wang Z, Xu X, Han W, Wang Q, Zou D. 2016. Leaf margin analysis of Chinese woody plants and the constraints on its application to palaeoclimatic reconstruction. Glob Ecol Biogeogr, 25: 1401–1415
Li Y, Liu C, Sack L, Xu L, Li M, Zhang J, He N. 2022. Leaf trait network architecture shifts with species-richness and climate across forests at continental scale. Ecol Lett, 25: 1442–1457
Linnemann U, Su T, Kunzmann L, Spicer R A, Ding W N, Spicer T E V, Zieger J, Hofmann M, Moraweck K, Gärtner A, Gerdes A, Marko L, Zhang S T, Li S F, Tang H, Huang J, Mulch A, Mosbrugger V, Zhou Z K. 2018. New U-Pb dates show a Paleogene origin for the modern Asian biodiversity hot spots. Geology, 46: 3–6
Liu Z H, Pagani M, Zinniker D, DeConto R, Huber M, Brinkhuis H, Shah S R, Leckie R M, Pearson A. 2009. Global cooling during the Eocene-Oligocene climate transition. Science, 323: 1187–1190
Mai D H, Walther H. 2000. Die Fundstellen eozäner Floren des Weißelster-Beckens und seiner Randgebiete. Altenb Naturwiss Forsch, 13: 1–59
McElwain J C, Yiotis C, Lawson T. 2016. Using modern plant trait relationships between observed and theoretical maximum stomatal conductance and vein density to examine patterns of plant macroevolution. New Phytol, 209: 94–103
Miller K G, Browning J V, Aubry M P, Wade B S, Katz M E, Kulpecz A A,

Wright J D. 2008. Eocene-Oligocene global climate and sea-level changes: St. Stephens Quarry, Alabama. GSA Bull, 120: 34–53
Moraweck K, Uhl D, Kunzmann L. 2015. Estimation of late Eocene (Bartonian-Priabonian) terrestrial palaeoclimate: Contributions from megafloral assemblages from central Germany. Palaeogeogr Palaeoclimatol Palaeoecol, 433: 247–258
Moraweck K, Grein M, Konrad W, Kvaček J, Kova-Eder J, Neinhuis C, Traiser C, Kunzmann L. 2019. Leaf traits of long-ranging Paleogene species and their relationship with depositional facies, climate and atmospheric CO_2 level. Palaeontograph Abteil B, 298: 93–172
Müller C, Toumoulin A, Böttcher H, Roth-Nebelsick A, Wappler T, Kunzmann L. 2023. An integrated leaf trait analysis of two Paleogene leaf floras. PeerJ, 11: e15140
Pagani M, Huber M, Liu Z, Bohaty S M, Henderiks J, Sijp W, Krishnan S, DeConto R M. 2011. The role of carbon dioxide during the onset of Antarctic glaciation. Science, 334: 1261–1264
Page M, Licht A, Dupont-Nivet G, Meijer N, Barbolini N, Hoorn C, Schauer A, Huntington K, Bajnai D, Fiebig J, Mulch A, Guo Z. 2019. Synchronous cooling and decline in monsoonal rainfall in northeastern Tibet during the fall into the Oligocene icehouse. Geology, 47: 203–206
Pan S, Liu C, Zhang W, Xu S, Wang N, Li Y, Gao J, Wang Y, Wang G. 2013. The scaling relationships between leaf mass and leaf area of vascular plant species change with altitude. PLoS ONE, 8: e76872
Pearson P N, Foster G L, Wade B S. 2009. Atmospheric carbon dioxide through the Eocene-Oligocene climate transition. Nature, 461: 1110–1113
Pound M J, Salzmann U. 2017. Heterogeneity in global vegetation and terrestrial climate change during the late Eocene to early Oligocene transition. Sci Rep, 7: 43386
Rahbek C, Borregaard M K, Antonelli A, Colwell R K, Holt B G, Nogues-Bravo D, Rasmussen C M Ø, Richardson K, Rosing M T, Whittaker R J, Fjeldså J. 2019. Building mountain biodiversity: Geological and evolutionary processes. Science, 365: 1114–1119
Roth-Nebelsick A, Grein M, Traiser C, Moraweck K, Kunzmann L, Kovar-Eder J, Kvaček J, Stiller S, Neinhuis C. 2017. Functional leaf traits and leaf economics in the Paleogene—A case study for Central Europe. Palaeogeogr Palaeoclimatol Palaeoecol, 472: 1–14
Royer D L, Peppe D J, Wheeler E A, Niinemets Ü. 2012. Roles of climate and functional traits in controlling toothed vs. untoothed leaf margins. Am J Bot, 99: 915–922
Sack L, Scoffoni C. 2013. Leaf venation: Structure, function, development, evolution, ecology and applications in the past, present and future. New Phytol, 198: 983–1000
Scher H D, Whittaker J M, Williams S E, Latimer J C, Kordesch W E C, Delaney M L. 2015. Onset of Antarctic circumpolar current 30 million years ago as Tasmanian Gateway aligned with westerlies. Nature, 523: 580–583
Scoffoni C, Rawls M, McKown A, Cochard H, Sack L. 2011. Decline of leaf hydraulic conductance with dehydration: Relationship to leaf size and venation architecture. Plant Physiol, 156: 832–843
Sheldon N D, Costa E, Cabrera L, Garcés M. 2012. Continental climatic and weathering response to the Eocene-Oligocene transition. J Geol, 120: 227–236
Song B W, Spicer R A, Zhang K X, Ji J L, Farnsworth A, Hughes A C, Yang Y B, Han F, Xu Y D, Spicer T, Shen T Y, Lunt D J, Shi G L. 2020. Qaidam Basin leaf fossils show northeastern Tibet was high, wet and cool in the early Oligocene. Earth Planet Sci Lett, 537: 116175
Sorrel P, Eymard I, Leloup P H, Maheo G, Olivier N, Sterb M, Gourbet L, Wang G C, Wu J, Lu H J, Li H B, Xu Y D, Zhang K X, Cao K, Chevalier M L, Replumaz A. 2017. Wet tropical climate in SE Tibet during the Late Eocene. Sci Rep, 7: 7809
Standke G, Escher D, Fischer J, Rascher J. 2010. The Tertiary Stratigraphic Sequence of Northwest Saxony (in German). Freiberg: Saxony State Office for Environment, Agriculture and Geology. 21–107
Su T, Xing Y W, Liu Y S, Jacques F M B, Chen W Y, Huang Y J, Zhou Z K. 2010. Leaf Margin Analysis: A new equation from humid to mesic forests in China. Palaios, 25: 234–238
Su T, Spicer R A, Li S H, Xu H, Huang J, Sherlock S, Huang Y J, Li S F, Wang L, Jia L B, Deng W Y D, Liu J, Deng C L, Zhang S T, Valdes P J, Zhou Z K. 2019. Uplift, climate and biotic changes at the Eocene-Oligocene transition in south-eastern Tibet. Natl Sci Rev, 6: 495–504
Sun B N, Wu J Y, Liu Y S C, Ding S T, Li X C, Xie S P, Yan D F, Lin Z C. 2011. Reconstructing Neogene vegetation and climates to infer tectonic uplift in western Yunnan, China. Palaeogeogr Palaeoclimatol Palaeoecol, 304: 328–336
Tang H, Li S F, Su T, Spicer R A, Zhang S T, Li S H, Liu J, Lauretano V, Witkowski C R, Spicer T E V, Deng W Y D, Wu M X, Ding W N, Zhou Z K. 2020. Early Oligocene vegetation and climate of southwestern China inferred from palynology. Palaeogeogr Palaeoclimatol Palaeoecol, 560: 109988
Tardif D, Toumoulin A, Fluteau F, Donnadieu Y, Le Hir G, Barbolini N, Licht A, Ladant J B, Sepulchre P, Viovy N, Hoorn C, Dupont-Nivet G. 2021. Orbital variations as a major driver of climate and biome distribution during the greenhouse to icehouse transition. Sci Adv, 7: eabh2819
Teodoridis V, Kvaček Z. 2015. Palaeoenvironmental evaluation of Cainozoic plant assemblages from the Bohemian Massif (Czech Republic) and adjacent Germany. Bull Geosci, 90: 695–720
Teodoridis V, Kovar-Eder J, Mazouch P. 2011a. Integrated plant record (Ipr) vegetation analysis applied to modern vegetation in south China and Japan. Palaios, 26: 623–638
Teodoridis V, Kovar-Eder J, Marek P, Kvaček Z, Mazouch P. 2011b. The integrated plant record vegetation analysis: Internet platform and online application. Acta Musei Natl Pragae Ser B, 67: 159–164
Teodoridis V, Kvaček Z, Zhu H, Mazouch P. 2012. Environmental analysis of the mid-latitudinal European Eocene sites of plant macrofossils and their possible analogues in East Asia. Palaeogeogr Palaeoclimatol Palaeoecol, 333-334: 40–58
Teodoridis V, Mazouch P, Kovar-Eder J. 2020. The Integrated Plant Record (IPR) analysis: Methodological advances and new insights into the evolution of European Palaeogene/Neogene vegetation. Palaeontol Electron, 23: 1–19
Tosal A, Sanjuan J, Cartanyà J, Martín-Closas C. 2018. Taphonomy and palaeoecology of the uppermost Eocene flora from Sarral (Eastern Ebro Basin): Palaeoclimatic implications. Palaeogeogr Palaeoclimatol Palaeoecol, 497: 66–81
Toumoulin A, Tardif D, Donnadieu Y, Licht A, Ladant J B, Kunzmann L, Guillaume G. 2022. Evolution of continental temperature seasonality from the Eocene greenhouse to the Oligocene icehouse—A model-data comparison. Clim Past, 18: 341–362
Wade B S, O'Neill J F, Phujareanchaiwon C, Ali I, Lyle M, Witkowski J. 2020. Evolution of deep-sea sediments across the Paleocene-Eocene and Eocene-Oligocene boundaries. Earth-Sci Rev, 211: 103403
Walls R L. 2011. Angiosperm leaf vein patterns are linked to leaf functions in a global-scale data set. Am J Bot, 98: 244–253
Walther H, Kvaček Z. 2007. Eearly Oligocene flora of Seifhennersdorf (Saxony). Acta Musei Natl Pragae Ser B, 63: 85–174
Wang W T, Zheng W J, Zhang P Z, Li Q, Kirby E, Yuan D Y, Zheng D W, Liu C C, Wang Z C, Zhang H P, Pang J Z. 2017. Expansion of the Tibetan Plateau during the Neogene. Nat Commun, 8: 15887
Westerhold T, Marwan N, Drury A J, Liebrand D, Agnini C, Anagnostou E, Barnet J S K, Bohaty S M, De Vleeschouwer D, Florindo F, Frederichs T, Hodell D A, Holbourn A E, Kroon D, Lauretano V, Littler K, Lourens L J, Lyle M, Pälike H, Röhl U, Tian J, Wilkens R H, Wilson P A, Zachos J C. 2020. An astronomically dated record of Earth's climate and its predictability over the last 66 million years. Science, 369: 1383–1387
Writing Group of Cenozoic Plant of China. 1978. Fossil Plants of China. Vol. 3: Cenozoic Plants from China (in Chinese). Beijing: Science Press. 177–183
Wu J, Zhang K X, Xu Y D, Wang G C, Garzione C N, Eiler J, Leloup P H, Sorrel P, Mahéo G. 2018. Paleoelevations in the Jianchuan Basin of the southeastern Tibetan Plateau based on stable isotope and pollen grain analyses. Palaeogeogr Palaeoclimatol Palaeoecol, 510: 93–108

Wu M X, Huang J, Spicer R A, Li S F, Zhao J G, Deng W Y D, Ding W N, Tang H, Xing Y W, Tian Y M, Zhou Z K, Su T. 2022. The early Oligocene establishment of modern topography and plant diversity on the southeastern margin of the Tibetan Plateau. Glob Planet Change, 214: 103856

Xie Y L, Wu F L, Fang X M, Song J Z, Niu Z C. 2022. Late Eocene onset of the East Asian Monsoon in the Qingjiang Basin of Central Jiangxi Province (Southeast China) revealed by a major vegetation transition from desert to forest. Palaeogeogr Palaeoclimatol Palaeoecol, 602: 111179

Xiong Z Y, Ding L, Spicer R A, Farnsworth A, Wang X, Valdes P J, Su T, Zhang Q H, Zhang L Y, Cai F L, Wang H Q, Li Z Y, Song P P, Guo X D, Yue Y H. 2020. The early Eocene rise of the Gonjo Basin, SE Tibet: From low desert to high forest. Earth Planet Sci Lett, 543: 116312

Yu X Q, Gao L M, Soltis D E, Soltis P S, Yang J B, Fang L, Yang S X, Li D Z. 2017. Insights into the historical assembly of East Asian subtropical evergreen broadleaved forests revealed by the temporal history of the tea family. New Phytol, 215: 1235–1248

Zachos J C, Quinn T M, Salamy K A. 1996. High-resolution (10^4 years) deep-sea foraminiferal stable isotope records of the Eocene-Oligocene climate transition. Paleoceanography, 11: 251–266

Zachos J C, Pagani M, Sloan L, Thomas E, Billups K. 2001. Trends, rhythms, and aberrations in global climate 65 Ma to Present. Science, 292: 686–693

Zhao C Y, Xiong Z Y, Farnsworth A, Spicer R A, He S L, Wang C, Zeng D, Cai F L, Wang H Q, Tian X L, Valdes P J, Lamu C, Xie J, Yue Y H, Ding L. 2023. The late Eocene rise of SE Tibet formed an Asian 'Mediterranean' climate. Glob Planet Change, 231: 104313

Zheng H B, Yang Q, Cao S, Clift P D, He M Y, Kano A, Sakuma A, Xu H, Tada R, Jourdan F. 2022. From desert to monsoon: Irreversible climatic transition at ~36 Ma in southeastern Tibetan Plateau. Prog Earth Planet Sci, 9: 12

Zhou Z K, Liu J, Chen L L, Spicer R A, Li S F, Huang J, Zhang S T, Huang Y J, Jia L B, Hu J J, Su T. 2023. Cenozoic plants from Tibet: An extraordinary decade of discovery, understanding and implications. Sci China Earth Sci, 66: 205–226

(Editorial handling: Yan ZHAO)